

Optimal molecular alignment and orientation through rotational ladder climbing

Julien Salomon*

*Laboratoire Jacques-Louis Lions, Université Pierre & Marie Curie,
Boîte courrier 187, 75252 Paris Cedex 05, France*

Claude M. Dion†

Department of Physics, Umeå University, SE-901 87 Umeå, Sweden

Gabriel Turinici‡

*INRIA Rocquencourt, B.P. 105, 78153 Le Chesnay Cedex and
CERMICS-ENPC, Champs-sur-Marne, 77455 Marne-la-Vallée Cedex, France*

(Dated: November 6, 2018)

We study the control by electromagnetic fields of molecular alignment and orientation, in a linear, rigid rotor model. With the help of a monotonically convergent algorithm, we find that the optimal field is in the microwave part of the spectrum and acts by resonantly exciting the rotation of the molecule progressively from the ground state, i.e., by rotational ladder climbing. This mechanism is present not only when maximizing orientation or alignment, but also when using prescribed target states that simultaneously optimize the efficiency of orientation/alignment and its duration. The extension of the optimization method to consider a finite rotational temperature is also presented.

I. INTRODUCTION

External fields can be used to manipulate molecules to achieve molecular axis alignment or orientation. Here, alignment refers to setting the molecular axis parallel to a laboratory fixed frame, while orientation implies that the molecular axis has in addition the same direction as the laboratory fixed frame. These two goals have a wide range of applications in fields such as chemical reactivity,¹ surface processing,^{2,3} nanoscale design,^{4,5} attosecond pulse production,^{6,7} and quantum information processing.⁸

Efficient alignment^{9,10} and orientation^{11,12} can be achieved by laser-induced adiabatic passage from field-free rotational states to aligned pendular states,^{13,14,15,16,17} but it is lost at the end of the laser pulse. Field-free alignment is possible by sudden excitation using pulses much shorter than the rotational period of the molecule.^{18,19,20,21,22} Achieving orientation with short pulses is more difficult since spatial symmetry breaking is required to give the direction of orientation, but it can be done using half-cycle pulses^{23,24} or specially tailored laser pulses.^{25,26} This has led to different proposals for alignment and orientation using series of short impulses (kicks).^{27,28,29,30,31,32,33,34} See also the recent review of the subject by Stapelfeldt and Seideman, and references therein.³⁵

The purpose of the present study is to find the electromagnetic fields that produce the best possible orientation or alignment. We start by presenting in Sec. II the rigid rotor model used to describe the rotation of a linear molecule, along with the cost functionals that describes the required control objectives, in terms of both observables measuring orientation or alignment and target states that embody the efficiency of orientation/alignment along with its persistence.

The optimization procedure itself is based on monotonically convergent algorithms^{36,37,38} that are guaranteed to improve at each step the cost functional chosen. The corresponding algorithm for the control of alignment/orientation is presented in Sec. II C.

As we will see in Sec. III, the fields leading to optimal orientation and alignment are in the microwave part of the spectrum and lead to *rotational ladder climbing*, i.e., the molecule is resonantly excited successively from one rotational level to the next. The possibility of controlling rotational excitation by ladder climbing using microwave fields was first proposed by Judson *et al.*^{39,40} A process similar but resting on Raman excitation of ro-vibrational states with chirped pulses has been used to create an optical centrifuge for molecules.^{41,42,43,44,45}

II. MODEL

A. Time-dependent Schrödinger equation

The dynamics of the molecule interacting with the electromagnetic field is obtained by solving the time-dependent Schrödinger equation (TDSE). We restrict ourselves to the case of a linear molecule in a rigid rotor approximation,

yielding the Hamiltonian (in atomic units, $\hbar = 1$)

$$\hat{H} = B\hat{J}^2 - \mu_0\mathcal{E}(t)\cos\theta - [(\alpha_{\parallel} - \alpha_{\perp})\cos^2\theta + \alpha_{\perp}]\frac{\mathcal{E}^2(t)}{2}, \quad (1)$$

where B is the rotational constant, \hat{J} is the angular momentum operator, θ is the polar angle positioning the molecular axis with respect to the polarization vector of the linearly polarized electric field of amplitude $\mathcal{E}(t)$, μ_0 is the permanent dipole moment, and α_{\parallel} and α_{\perp} are the dipole polarizability components parallel and perpendicular to the molecular axis, respectively. Because of the cylindrical symmetry about the field polarization axis, the motion associated with the azimuthal angle can be separated and M , the projection of the total angular momentum J on the axis, is a good quantum number ($\Delta M = 0$). The TDSE (1) is solved numerically starting from the ground rotational (isotropic) state $J = M = 0$, using a basis set expansion of the wave function ψ in terms of the spherical harmonics $Y_{J,M}$,

$$\psi(\theta, t) = \sum_{J=0}^{\infty} c_J(t)Y_{J,0}(\theta), \quad (2)$$

the c_J being complex coefficients and the coupling terms due to μ_0 and α being then analytical.⁴⁶ For computational purposes, only the first 10 terms in the sum in Eq. (2) are kept, and we have checked that the results are not affected by using a bigger basis.

Because of the presence of both the dipole moment μ and the polarizability anisotropy $\Delta\alpha \equiv \alpha_{\parallel} - \alpha_{\perp}$, the results are not molecule-independent. However, the role of the polarizability is negligible for the fields obtained, making them applicable to any linear molecule with a proper scaling of the amplitude and frequency of the electric field. The results will thus be presented with time expressed in units of the rotational period $T_{\text{rot}} = h/2B$, the electrical field as $\mu_0\mathcal{E}/B$, and energy as E/B . The parameters actually used in the calculations are those for the HCN molecule: $B = 6.6376 \times 10^{-6}$, $\mu = 1.1413$, $\alpha_{\parallel} = 20.055$, and $\alpha_{\perp} = 8.638$ (all in atomic units).

B. Cost functional

As we are seeking to optimize molecular orientation or alignment, our cost functionals are based on their respective measure, the expectation values $\langle \cos\theta \rangle$ and $\langle \cos^2\theta \rangle$. A molecule will be oriented when $|\langle \cos\theta \rangle| \sim 1$, with the sign indicating in which direction it is pointing; an angular distribution symmetric with respect to $\theta = \pi/2$ will yield a value of zero. The expectation value of $\cos^2\theta$ is 1 when the molecule is aligned, starting from 1/3 for the isotropic case.

The first case we consider is a cost functional of the form

$$\mathcal{J}_1(\mathcal{E}) = \langle \psi(t_f) | \hat{O} | \psi(t_f) \rangle - \int_0^{t_f} \lambda(t)\mathcal{E}^2(t) dt, \quad (3)$$

with \hat{O} an operator chosen to be $\cos\theta + \hat{I}$ for orientation and $\cos^2\theta + \hat{I}$ for alignment, the identity operator \hat{I} being used for convenience (e.g., it ensures that \hat{O} is positive) without modifying the extrema of \mathcal{J}_1 , and t_f the time at which the interaction with the field ends. The last term in Eq. (3) is a penalization on the amplitude of the field, with

$$\lambda(t) = 10^5 \left(\frac{t - t_f/2}{t_f/2} \right)^6 + 10^4. \quad (4)$$

This imposes a strong constraint on the maximum amplitude of the electric field, such that the field strengths are comparable to those that can be achieved for half-cycle pulses,^{47,48} allowing a comparison with previously published results for alignment and orientation using kicks.^{23,24,27,28,29,30,31,32,33,34} In addition, the form of Eq. (4) ensures a smoother, and thus more realistic, turn-on and turn-off of the field. We point out that, in any case, this penalty term is not an essential ingredient of the monotonic algorithm and can be relaxed (e.g., to allow fluences achievable with laser pulses) or completely eliminated.

The downside of such a cost functional is that it takes into account only the efficiency of the orientation/alignment, not its persistence. Once the field is turned off, the free rotation of the molecule will lead to the disappearance of the orientation/alignment as the different J components in the wave function dephase, followed by revivals at intervals of one rotational period.¹⁹ The best orientation/alignment is obtained by confining the molecule to a narrow angular distribution $\Delta\theta$, which corresponds to exciting a broad rotational band ΔJ by referring to an uncertainty principle $\Delta J \cdot \Delta\theta \sim \hbar$.³⁵ The problem is then that, conversely, a broad rotational spectrum exhibits narrow features in the time

domain, i.e., the greater the orientation/alignment, the shorter its duration. A compromise has thus to be made, as can be achieved by considering the best orientation/alignment possible for a restricted maximum rotational excitation. The procedure on how states with such characteristics can be obtained is given in detail in Refs. 34,49, where it can also be seen that $J_{\max} = 4$ offers a good compromise, leading to an orientation of $\langle \cos \theta \rangle \approx 0.906$ or an alignment of $\langle \cos^2 \theta \rangle \approx 0.837$, both lasting of the order of 1/10th of the rotational period. The cost functional is now

$$\mathcal{J}_2(\mathcal{E}) = 2\Re \langle \psi_{\text{target}} | \psi(t_f) \rangle - \int_0^{t_f} \lambda(t) \mathcal{E}^2(t) dt, \quad (5)$$

where ψ_{target} denotes the target state corresponding to orientation or alignment, as given in Table I, and \Re the real part. Note that because of the norm conservation properties of the Schrödinger equation, the cost functional (5) has the same minima and critical points as

$$\mathcal{J}(\mathcal{E}) = - \|\psi_{\text{target}} - \psi(t_f)\|^2 - \int_0^{t_f} \lambda(t) \mathcal{E}^2(t) dt, \quad (6)$$

which measures the distance between ψ_{target} and $\psi(t_f)$.

In all cases, the time at which the field is turned off and the cost functional measured is chosen as $t_f = 9.5 \times 10^6$ a.u. $\approx 20T_{\text{rot}}$ for the results presented here. Shorter durations lead to results either similar or less significant.

C. Monotonically convergent algorithm

The algorithm used to find the optimal field is based on a general class of monotonically convergent algorithms recently proposed.³⁸ We present here the algorithm associated to \mathcal{J}_1 and refer the reader to Refs. 50,51 for a detailed discussion the algorithm in a time-discretized framework. At the maximum of the cost functional \mathcal{J}_1 , the Euler-Lagrange critical point equations are satisfied; a standard way to write these equations is to use a Lagrange multiplier $\chi(\theta, t)$ called *adjoint state*. The following critical point equations are thus obtained:

$$\begin{aligned} i\partial_t \psi &= \hat{H}\psi, & \psi(0) &= \psi_0, \\ i\partial_t \chi &= \hat{H}\chi, & \chi(t_f) &= \hat{O}(\psi(t_f)), \\ \lambda(t)\mathcal{E}(t) &= -\Im \langle \chi(t) | \mu_0 \cos \theta + 2\mathcal{E}(t) (\Delta\alpha \cos^2 \theta + \alpha_{\perp}) | \psi(t) \rangle, \end{aligned} \quad (7)$$

where \Im is the imaginary part of a complex number and ψ_0 the initial state of the controlled system.

Given two fields \mathcal{E} and \mathcal{E}' and the corresponding states ψ, ψ' and adjoint states χ, χ' defined by Eq. (7), one can write

$$\begin{aligned} \Delta\mathcal{J}_1 &= \mathcal{J}_1(\mathcal{E}') - \mathcal{J}_1(\mathcal{E}) \\ &= \langle \psi'(t_f) - \psi(t_f) | \hat{O} | \psi'(t_f) - \psi(t_f) \rangle \\ &\quad + \int_0^{t_f} [\mathcal{E}'(t) - \mathcal{E}(t)] \left\{ 2\Im \langle \psi'(t) | \mu_0 \cos \theta | \chi(t) \rangle \right. \\ &\quad \left. + [\mathcal{E}'(t) + \mathcal{E}(t)] \left[2\Im \langle \psi'(t) | \frac{\Delta\alpha \cos^2 \theta + \alpha_{\perp}}{2} | \chi(t) \rangle - \lambda(t) \right] \right\} dt. \end{aligned} \quad (8)$$

The first term of this sum is positive since both choices $\hat{O} = \cos + \hat{I}$ or $\hat{O} = \cos^2 + \hat{I}$ are positive. Given \mathcal{E} , the integrand provides thus an implicit criterion in terms of \mathcal{E}' , the satisfaction of which guarantees the positivity of $\Delta\mathcal{J}_1$. An explicit choice of \mathcal{E}' can be exhibited: the integrand of Eq. (8) is a second-order polynomial with respect to \mathcal{E}' and for a large enough value of $\lambda(t)$ the coefficient $2\Im \langle \psi'(t) | \frac{\Delta\alpha \cos^2 \theta + \alpha_{\perp}}{2} | \chi(t) \rangle - \lambda(t)$ of $\mathcal{E}'^2(t)$ is negative. It has thus a unique maximum, given by the cancellation of the derivative. The value obtained by this method is

$$\mathcal{E}'(t) = - \frac{\Im \langle \psi'(t) | \mu_0 \cos \theta | \chi(t) \rangle}{2\Im \langle \psi'(t) | \frac{\Delta\alpha \cos^2 \theta + \alpha_{\perp}}{2} | \chi(t) \rangle - \lambda(t)}. \quad (9)$$

The algorithm derived from the previous computations is then given by the following procedure: given at step k a field \mathcal{E}^k and its associated state ψ^k and adjoint state χ^k , compute simultaneously $\mathcal{E}^{k+1}, \psi^{k+1}$ by

$$\begin{cases} \mathcal{E}^{k+1}(t) = - \frac{\Im \langle \psi^{k+1}(t) | \mu_0 \cos \theta | \chi^k(t) \rangle}{2\Im \langle \psi^{k+1}(t) | \frac{\Delta\alpha \cos^2 \theta + \alpha_{\perp}}{2} | \chi^k(t) \rangle - \lambda(t)}, \\ i\partial_t \psi^{k+1}(t) = \left[B - \mu_0 \mathcal{E}^{k+1}(t) \cos \theta - \frac{[\mathcal{E}^{k+1}(t)]^2}{2} (\Delta\alpha \cos^2 \theta + \alpha_{\perp}) \right] \psi^{k+1}(t), \\ \psi^{k+1}(\theta, t=0) = \psi_0(\theta). \end{cases} \quad (10)$$

Then compute backward evolution of χ^{k+1} by

$$\begin{cases} i\partial_t \chi^{k+1}(t) = \left[B - \mu_0 \mathcal{E}^{k+1}(t) \cos \theta - \frac{[\mathcal{E}^{k+1}(t)]^2}{2} (\Delta\alpha \cos^2 \theta + \alpha_\perp) \right] \chi^{k+1}(t), \\ \chi^{k+1}(\theta, t_f) = \hat{O}(\psi^{k+1}(\theta, t_f)). \end{cases} \quad (11)$$

The arguments above show that

$$\mathcal{J}_1(\mathcal{E}^{k+1}) \geq \mathcal{J}_1(\mathcal{E}^k). \quad (12)$$

III. RESULTS

A. Optimizing orientation

The electric field obtained using the cost functional \mathcal{J}_1 [Eq. (3)] with the observable $\hat{O} = \cos \theta + \hat{I}$, i.e., for the optimization of the orientation, is given in Fig. 1(a). To better analyze the result, we have performed a short-time Fourier transform (STFT),⁵²

$$\mathcal{F}(\nu, t) = \int_{-\infty}^{+\infty} \mathcal{E}(\tau) w(\tau - t) e^{-i2\pi\nu\tau} d\tau, \quad (13)$$

where w is a Tukey-Hanning window with a temporal width of 1.9×10^6 a.u. The frequency distribution \mathcal{F} can be seen in Fig. 1(b), where the ordinate is the dimensionless value $2\nu T_{\text{rot}}$, corresponding to the dimensionless energy E/B . The energy spacing between rotational states J and $J + 1$ being $2BJ$, we see clearly from Fig. 1(b) that the field is initially resonant with the $J = 0 \rightarrow 1$ transition, and subsequently comes in resonance with higher and higher pairs of rotational levels $J = 1 \rightarrow 2$, $J = 2 \rightarrow 3$, ... Looking at the population of the rotational states, in Fig. 2, we indeed find that, starting from the ground state $J = 0$, the molecule is pumped to the first excited state, then to the second, etc. At the end of interaction with the field, the population distribution is such that an orientation of $\langle \cos \theta \rangle(t_f) = 0.909$ is attained (Fig. 3). In other words, the molecule is oriented by a process of *rotational ladder climbing*.

If we instead take the cost functional \mathcal{J}_2 [Eq. (5)] with ψ_{target} the target state for orientation given in Table I, we obtain a result very similar to the previous one, as shown in Fig. 4. The main difference is the absence of the frequency component at $2\nu T_{\text{rot}} = 10$, which is easily understood from the fact that it corresponds to the $J = 4 \rightarrow 5$ transition, while the target is restricted to $J_{\text{max}} = 4$. The resulting dynamics of $\langle \cos \theta \rangle$ are nearly indistinguishable, as is seen in Fig. 5. The similarity of both results can also be explained by looking at the projection on the target $P \equiv |\langle \psi_{\text{target}} | \psi(t_f) \rangle|^2$. For the wave function obtained for the optimization of the observable, we already have $P = 0.9933$, the optimization of the projection on the target allowing to reach $P = 0.9969$. This efficiency is better than that obtained when kicking the molecule with short pulses,^{34,53} but the time necessary to reach the optimized state is of the order of 20 rotational periods, while it takes less than one molecular rotation with kicks. The time needed for ladder climbing also explains why the state reached for the optimization of $\langle \cos \theta \rangle$ is almost the same as the target state, since the time limit imposed by t_f constrains the maximum value of J than can be excited. It can be likened to the reduced Hilbert space used when defining the target state.^{34,49}

B. Optimizing alignment

The result for the maximization of the operator $\hat{O} = \cos^2 \theta + \hat{I}$ to achieve alignment is given in Fig. 6. The field obtained is almost the same as the one obtained for orientation, except that the rotational excitation happens at a quicker pace, as displayed in Fig. 7, where it is seen that $J = 5$ is now significantly populated. The alignment obtained is $\langle \cos^2 \theta \rangle = 0.866$.

Changing now the target state for alignment (Table I), we see in Fig. 8 that the field obtained is significantly different. The frequency component corresponding to an energy of $E = 4B$ is present for a longer time and components at $E = 6B$ and, to a lesser extent, $E = 2B$, reappear near the turn-off of the field. The time dependence of the population of the rotational states in Fig. 9 gives the explanation of this phenomenon: the populations of $J = 1$ and 3 are *pumped down* by these later components, since only even J levels are populated in the optimally aligned target state. The original excitation to the odd levels was necessary as the rotational states are only significantly coupled via the permanent dipole moment, implying the selection rule $\Delta J = \pm 1$, the role of the polarizability being here

negligible. This excitation-deexcitation scheme leads to a projection on the target state of $P = 0.9950$, compared with $P = 0.5487$ when only optimizing for alignment.

It is interesting to note that the maximum alignment obtained is the same as in the first case, with $\langle \cos^2 \theta \rangle (t_f) = 0.867$ (Fig. 10), even though the two wave functions obtained involve very different mixtures of spherical harmonics. One striking contrast between the two is actually not visible when looking only at $\langle \cos^2 \theta \rangle$: in the second case, the state obtained is *strictly* aligned, in the sense that the angular distribution is symmetric with respect to $\theta = \pi/2$. In the first case, the maximum in alignment corresponds also to a maximum in orientation, with $\langle \cos \theta \rangle (t_f) = 0.891$, whereas in the second case $\langle \cos \theta \rangle (t_f) = -0.027$.

C. Considering a rotational temperature

By starting all simulations from the ground rotational state, we have in fact made the approximation of a zero initial rotational temperature. From previous work on laser-induced alignment and orientation,^{15,24,25,54,55} it is known that considering a higher, experimentally more realistic initial rotational temperature will lead to an important decrease in the amount of orientation/alignment obtained. This can be seen in Fig. 11, where we show how orientation is affected when the optimal field presented in Fig. 1(a) is applied to a thermal ensemble of initial temperature $k_B T/B \approx 4.77$ (corresponding to 10 K for HCN).

This difficulty can be overcome by adapting the optimization method to take into account the initial thermal distribution.^{46,56} We present here the optimization of orientation, which can be trivially extended to the case of alignment or of a suitable mixed-state target.⁵⁷ The measure of orientation now reads

$$\langle \langle \cos \theta \rangle \rangle (t) = Q^{-1} \sum_{J=0}^{\infty} \exp \left[\frac{-BJ(J+1)}{k_B T} \right] \sum_{M=-J}^J \langle \cos \theta \rangle_{J,M} (t), \quad (14)$$

where

$$Q = \sum_{J=0}^{\infty} (2J+1) \exp \left[\frac{-BJ(J+1)}{k_B T} \right] \quad (15)$$

is the partition function and $\langle \cos \theta \rangle_{J,M} (t) \equiv \langle \psi_{J,M}(\theta; t) | \cos \theta | \psi_{J,M}(\theta; t) \rangle$ is obtained by solving the TDSE with the Hamiltonian (1) for the initial condition $\psi_{J,M}(\theta; t=0) \equiv Y_{J,M}(\theta)$. Considering a temperature $k_B T/B \approx 4.77$, we can restrict the sum over J in Eq. (14) to $J_{\max} = 7$, with 16 basis functions [see Eq. (2)] used for the time evolution. The monotonic algorithm (10) becomes

$$\begin{cases} \mathcal{E}^{k+1}(t) = -Q^{-1} \sum_{J=0}^{J_{\max}} \exp \left[\frac{-BJ(J+1)}{k_B T} \right] \sum_{M=-J}^J \frac{\Im \langle \psi_{J,M}^{k+1}(t) | \mu_0 \cos \theta | \chi_{J,M}^k(t) \rangle}{2 \Im \langle \psi_{J,M}^{k+1}(t) | \frac{\Delta \alpha \cos^2 \theta + \alpha_{\perp}}{2} | \chi_{J,M}^k(t) \rangle - \lambda(t)}, \\ i \partial_t \psi_{J,M}^{k+1}(t) = \left[B - \mu_0 \mathcal{E}^{k+1}(t) \cos \theta - \frac{[\mathcal{E}^{k+1}(t)]^2}{2} (\Delta \alpha \cos^2 \theta + \alpha_{\perp}) \right] \psi_{J,M}^{k+1}(t), \\ \psi_{J,M}^{k+1}(\theta, t=0) = Y_{J,M}(\theta). \end{cases} \quad (16)$$

The resulting optimized field, given in Fig. 12(a), allows to reach $\langle \langle \cos \theta \rangle \rangle (t_f) = 0.686$, which is much better than the value of 0.434 obtained when the $T = 0$ K field is applied to the same thermal distribution, as shown in Fig. 11. Looking at the Fourier transform of the field, Fig. 12(b), we see that the mechanism to achieve orientation is slightly different, with the lower frequencies present for a much longer time than previously observed, which reflects the fact that many $J \neq 0$ states are initially populated. Nevertheless, the ladder climbing structure of the resonances is still present.

IV. CONCLUSION

Using a monotonically convergent algorithm, we have searched for the optimal electric field maximizing either the alignment or the orientation of a linear molecule, taken in a rigid rotor approximation. We have carried out the optimization both in terms of maximization of observables corresponding to orientation/alignment and using target states offering a good compromise between the efficiency of orientation/alignment and its duration.

We have found that, starting from the ground rotational state, the optimal fields allow to reach orientation/alignment by rotational ladder climbing, i.e., by successive resonant excitation of neighboring rotational levels.

We insist on the fact that this scenario appears “naturally” from the physics of the problem and is not imposed *a priori* by the optimization algorithm. This process allows to reach an orientation of $\langle \cos \theta \rangle = 0.909$ or an alignment of $\langle \cos^2 \theta \rangle = 0.867$. Target states can also be reached to within better than 0.5%.

We have also shown how our optimization method can be extended to the more realistic case of an initial thermal distribution of rotational states. Using orientation as an illustrative example, we obtained a value of $\langle \langle \cos \theta \rangle \rangle = 0.686$ at a temperature $k_B T/B \approx 4.77$ (corresponding to 10 K for HCN). This result is much better than those previously reported,⁴⁶ even though we are considering here a *higher* rotational temperature.

As a rigid rotor model was used, this study did not take into account any vibrational excitation, which could hinder or enhance the orientation/alignment obtained. By including vibrations into the model, it is possible to use different control paths not involving direct rotational excitation, enabling the choice of infra-red lasers as control fields.^{21,58,59} Vibration-rotation coupling can also lead to cross-revivals of vibrational wave packets.^{60,61} Future work will thus take into account the vibration of the molecule.

Acknowledgments

We thank Yvon Maday and Arne Keller for stimulating discussions. Financial support from the *Action Concertée Incitative Nouvelles Interfaces des Mathématiques* is gratefully acknowledged.

-
- * Electronic address: salomon@ann.jussieu.fr
 † Electronic address: claude.dion@tp.umu.se
 ‡ Electronic address: Gabriel.Turinici@dauphine.fr
- ¹ P. R. Brooks, *Science* **193**, 11 (1976).
 - ² M. G. Tenner, E. W. Kuipers, A. W. Kleyn, and S. Stolte, *J. Chem. Phys.* **94**, 5197 (1991).
 - ³ J. J. McClelland, R. E. Scjoltjen, E. C. Palm, and R. J. Celotta, *Science* **262**, 877 (1993).
 - ⁴ T. Seideman, *Phys. Rev. A* **56**, R17 (1997).
 - ⁵ B. K. Dey, M. Shapiro, and P. Brumer, *Phys. Rev. Lett.* **85**, 3125 (2000).
 - ⁶ A. D. Bandrauk and H. Z. Lu, *Phys. Rev. A* **68**, 043408 (2003).
 - ⁷ R. de Nalda, E. Heesel, M. Lein, N. Hay, R. Velotta, E. Springate, M. Castillejo, and J. P. Marangos, *Phys. Rev. A* **69**, 031804(R) (2004).
 - ⁸ K. F. Lee, D. M. Villeneuve, P. B. Corkum, and E. A. Shapiro, *Phys. Rev. Lett.* **93**, 233601 (2004).
 - ⁹ H. Sakai, C. P. Safvan, J. J. Larsen, K. M. Hilligsøe, K. Hald, and H. Stapelfeldt, *J. Chem. Phys.* **110**, 10235 (1999).
 - ¹⁰ J. J. Larsen, H. Sakai, C. P. Safvan, I. Wendt-Larsen, and H. Stapelfeldt, *J. Chem. Phys.* **111**, 7774 (1999).
 - ¹¹ T. Kanai and H. Sakai, *J. Chem. Phys.* **115**, 5492 (2001).
 - ¹² S. Guérin, L. P. Yatsenko, H. R. Jauslin, O. Faucher, and B. Lavorel, *Phys. Rev. Lett.* **88**, 233601 (2002).
 - ¹³ B. A. Zon and B. G. Katsnel'son, *Sov. Phys. JETP* **42**, 595 (1975), [*Zh. Eksp. Teor. Fiz.* **69**, 1166 (1975)].
 - ¹⁴ B. Friedrich and D. Herschbach, *Phys. Rev. Lett.* **74**, 4623 (1995).
 - ¹⁵ J. Ortigoso, M. Rodríguez, M. Gupta, and B. Friedrich, *J. Chem. Phys.* **110**, 3870 (1999).
 - ¹⁶ A. I. Andryushin and M. V. Fedorov, *Sov. Phys. JETP* **89**, 837 (1999), [*Zh. Eksp. Teor. Fiz.* **116**, 1551 (1999)].
 - ¹⁷ A. Keller, C. M. Dion, and O. Atabek, *Phys. Rev. A* **61**, 023409 (2000).
 - ¹⁸ T. Seideman, *J. Chem. Phys.* **103**, 7887 (1995).
 - ¹⁹ T. Seideman, *Phys. Rev. Lett.* **83**, 4971 (1999).
 - ²⁰ N. E. Henriksen, *Chem. Phys. Lett.* **312**, 196 (1999).
 - ²¹ C. M. Dion, A. Keller, O. Atabek, and A. D. Bandrauk, *Phys. Rev. A* **59**, 1382 (1999).
 - ²² V. Renard, M. Renard, S. Guérin, Y. T. Pashayan, B. Lavorel, O. Faucher, and H. R. Jauslin, *Phys. Rev. Lett.* **90**, 153601 (2003).
 - ²³ C. M. Dion, A. Keller, and O. Atabek, *Eur. Phys. J. D* **14**, 249 (2001).
 - ²⁴ M. Machholm and N. E. Henriksen, *Phys. Rev. Lett.* **87**, 193001 (2001).
 - ²⁵ C. M. Dion, A. Ben Haj-Yedder, E. Cancès, C. Le Bris, A. Keller, and O. Atabek, *Phys. Rev. A* **65**, 063408 (2002).
 - ²⁶ O. Atabek, C. M. Dion, and A. Ben Haj Yedder, *J. Phys. B: At., Mol. Opt. Phys.* **36**, 4667 (2003).
 - ²⁷ I. S. Averbukh and R. Arvieu, *Phys. Rev. Lett.* **87**, 163601 (2001).
 - ²⁸ M. Leibscher, I. S. Averbukh, and H. Rabitz, *Phys. Rev. Lett.* **90**, 213001 (2003).
 - ²⁹ A. Matos-Abiague and J. Berakdar, *Phys. Rev. A* **68**, 063411 (2003).
 - ³⁰ J. Ortigoso, *Phys. Rev. Lett.* **93**, 073001 (2004).
 - ³¹ M. Leibscher, I. S. Averbukh, and H. Rabitz, *Phys. Rev. A* **69**, 013402 (2004).
 - ³² K. F. Lee, I. V. Litvinyuk, P. W. Dooley, M. Spanner, D. M. Villeneuve, and P. B. Corkum, *J. Phys. B: At., Mol. Opt. Phys.* **37**, L43 (2004).
 - ³³ C. Z. Bisgaard, M. D. Poulsen, E. Péronne, S. S. Viftrup, and H. Stapelfeldt, *Phys. Rev. Lett.* **92**, 173004 (2004).
 - ³⁴ D. Sugny, A. Keller, O. Atabek, D. Daems, C. M. Dion, S. Guérin, and H. R. Jauslin, *Phys. Rev. A* **69**, 033402 (2004).

- ³⁵ H. Stapelfeldt and T. Seideman, *Rev. Mod. Phys.* **75**, 543 (2003).
- ³⁶ D. Tannor, V. Kazakov, and V. Orlov, in *Time Dependent Quantum Molecular Dynamics*, edited by J. Broeckhove and L. Lathouwers (Plenum Press, New York, 1992), pp. 347–360.
- ³⁷ W. Zhu and H. Rabitz, *J. Chem. Phys.* **109**, 385 (1998).
- ³⁸ Y. Maday and G. Turinici, *J. Chem. Phys.* **118**, 8191 (2003).
- ³⁹ R. S. Judson, K. K. Lehmann, H. Rabitz, and W. S. Warren, *J. Mol. Spectrosc.* **223**, 425 (1990).
- ⁴⁰ R. S. Judson and H. Rabitz, *Phys. Rev. Lett.* **68**, 1500 (1992).
- ⁴¹ J. Karczmarek, J. Wright, P. Corkum, and M. Ivanov, *Phys. Rev. Lett.* **82**, 3420 (1999).
- ⁴² D. M. Villeneuve, S. A. Aseyev, P. Dietrich, M. Spanner, M. Y. Ivanov, and P. B. Corkum, *Phys. Rev. Lett.* **85**, 542 (2000).
- ⁴³ M. Spanner and M. Y. Ivanov, *J. Chem. Phys.* **114**, 3456 (2001).
- ⁴⁴ M. Spanner, K. M. Davitt, and M. Y. Ivanov, *J. Chem. Phys.* **115**, 8403 (2001).
- ⁴⁵ N. V. Vitanov and B. Girard, *Phys. Rev. A* **69**, 033409 (2004).
- ⁴⁶ A. Ben Haj-Yedder, A. Auger, C. M. Dion, E. Cancès, A. Keller, C. Le Bris, and O. Atabek, *Phys. Rev. A* **66**, 063401 (2002).
- ⁴⁷ D. You, R. R. Jones, P. H. Bucksbaum, and D. R. Dykaar, *Opt. Lett.* **18**, 290 (1993).
- ⁴⁸ P. Bucksbaum, in *The Physics and Chemistry of Wave Packets*, edited by J. A. Yeazell and T. Uzer (Wiley, New York, 2000).
- ⁴⁹ D. Sugny, A. Keller, O. Atabek, D. Daems, C. M. Dion, S. Guérin, and H. R. Jauslin, *Phys. Rev. A* **71**, 063402 (2005).
- ⁵⁰ Y. Maday, J. Salomon, and G. Turinici, in *Proceedings of the LHMNLC03 IFAC Conference* (2003), pp. 321–324.
- ⁵¹ Y. Maday, J. Salomon, and G. Turinici, *Numer. Math.* (to be published).
- ⁵² M. B. Priestley, *Spectral Analysis and Time Series* (Academic Press, San Diego, 1981).
- ⁵³ C. M. Dion, A. Keller, and O. Atabek, *Phys. Rev. A* (to be published), arXiv:physics.chem-ph/0505060.
- ⁵⁴ T. Seideman, *J. Chem. Phys.* **115**, 5965 (2001).
- ⁵⁵ M. Machholm, *J. Chem. Phys.* **115**, 10724 (2001).
- ⁵⁶ G. Turinici and H. Rabitz, *Phys. Rev. A* **70**, 063412 (2004).
- ⁵⁷ D. Sugny, A. Keller, O. Atabek, D. Daems, C. M. Dion, S. Guérin, and H. R. Jauslin, (unpublished).
- ⁵⁸ C. M. Dion, A. D. Bandrauk, O. Atabek, A. Keller, H. Umeda, and Y. Fujimura, *Chem. Phys. Lett.* **302**, 215 (1999).
- ⁵⁹ K. Hoki and Y. Fujimura, *Chem. Phys.* **267**, 187 (2001).
- ⁶⁰ T. Hansson, *Phys. Rev. A* **61**, 033404 (2000).
- ⁶¹ S. Wallentowitz, I. A. Walmsley, L. J. Waxer, and T. Richter, *J. Phys. B: At., Mol. Opt. Phys.* **35**, 1967 (2002).

J	c_J^o	c_J^a
0	0.344185	0.413914
1	0.540216	0.
2	0.563165	0.744364
3	0.456253	0.
4	0.253736	0.524021

TABLE I: Expansion coefficients [see Eq. (2)] for the target states ψ_{target} corresponding to maximum orientation, c_J^o , and alignment, c_J^a , when the rotational excitation is restricted to $J_{\text{max}} = 4$.

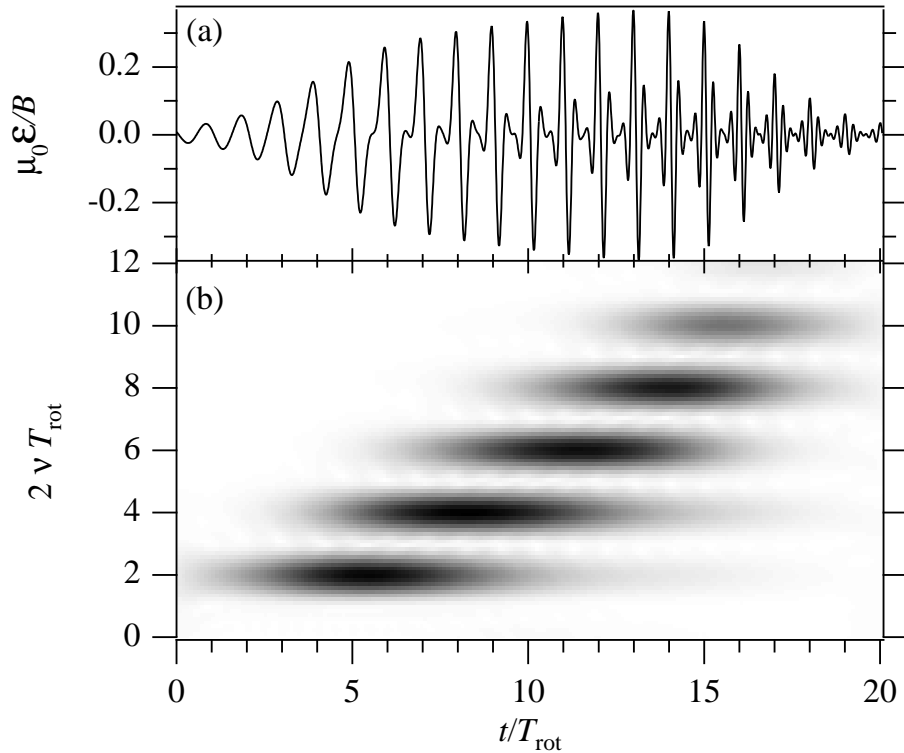


FIG. 1: (a) Electric field obtained with criterion \mathcal{J}_1 for the optimization of $\langle \cos \theta \rangle$. (b) Short-time Fourier transform of the field in (a).

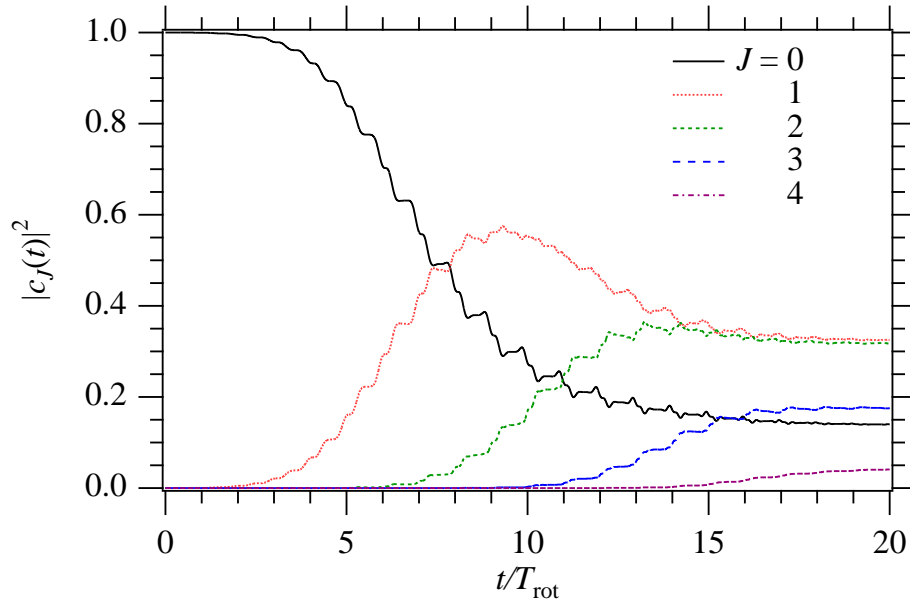


FIG. 2: Time evolution of the population of rotational states of a rigid rotor interacting with the electric field given in Fig. 1(a).

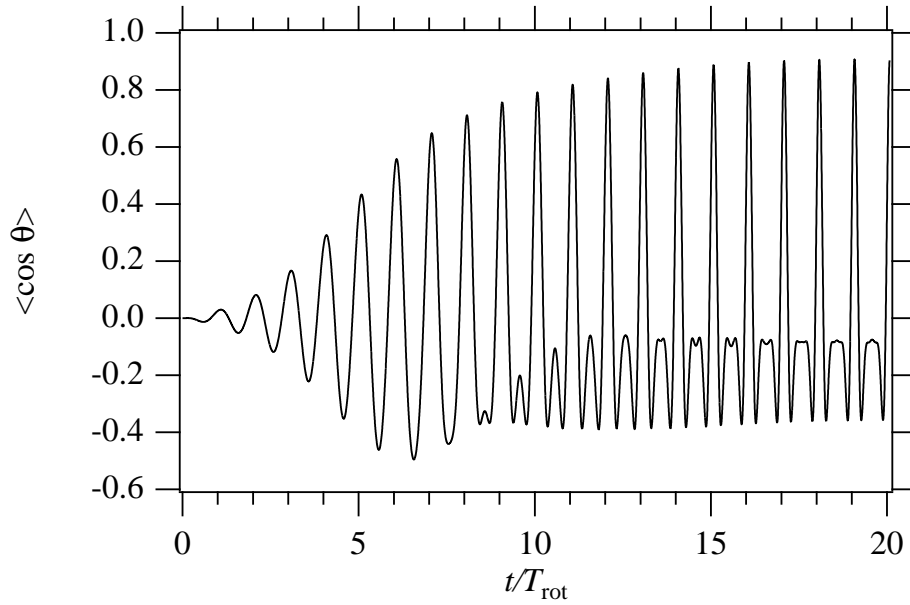


FIG. 3: Orientation, as measured by $\langle \cos \theta \rangle$, obtained for a rigid rotor interacting with the electric field given in Fig. 1(a). The field-free evolution is then periodic with period T_{rot} .

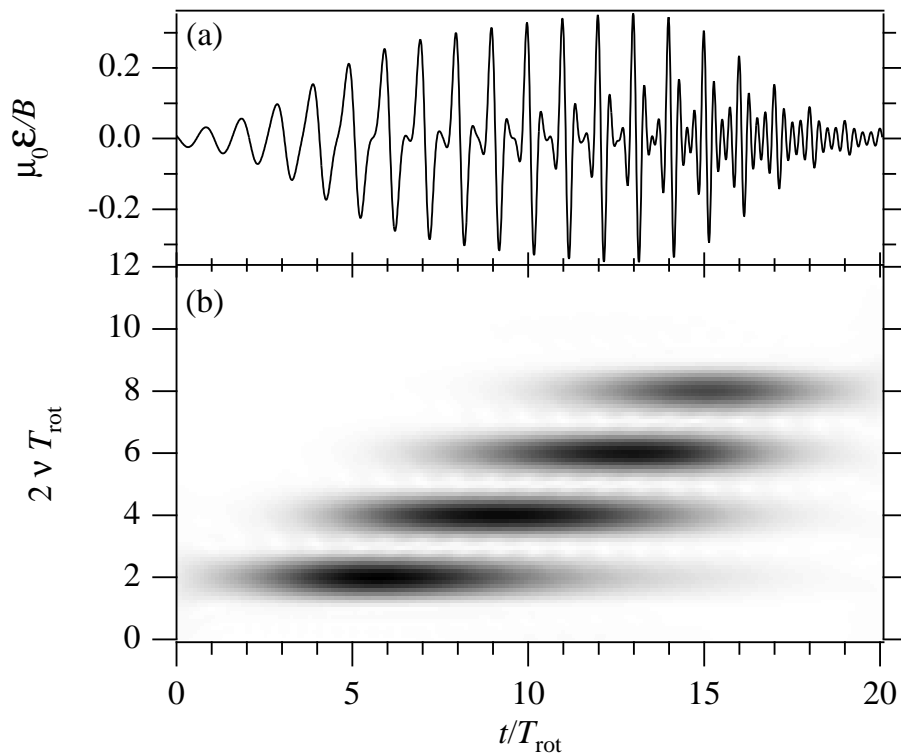


FIG. 4: (a) Electric field obtained with criterion \mathcal{J}_2 for the optimization of the projection of wave function on the target ψ_{target} corresponding to orientation (see Table I). (b) Short-time Fourier transform of the field in (a).

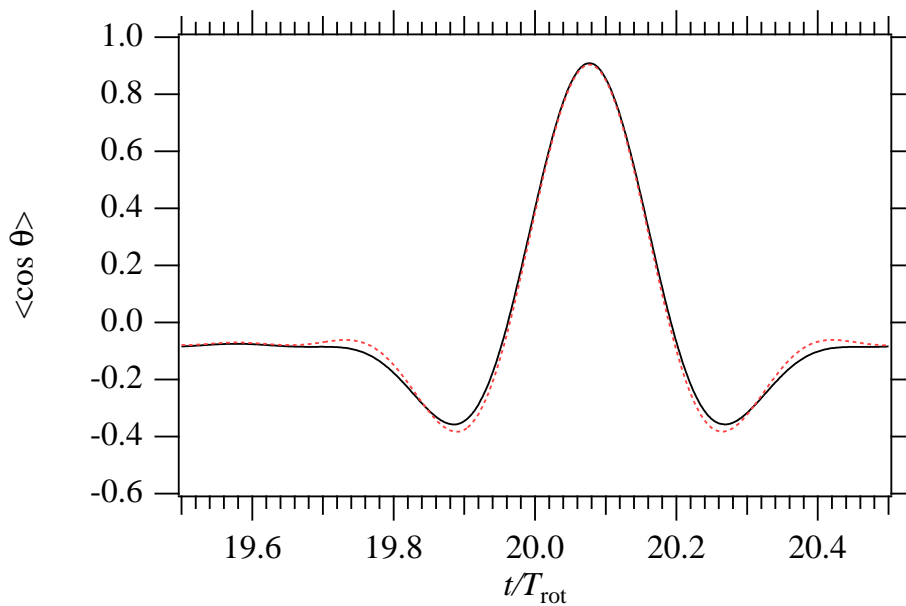


FIG. 5: Orientation, as measured by $\langle \cos \theta \rangle$, obtained for the interaction with the electric field given in Fig. 1(a) (solid line) and Fig. 4(a) (dashed line). The field-free evolution is then periodic with period T_{rot} .

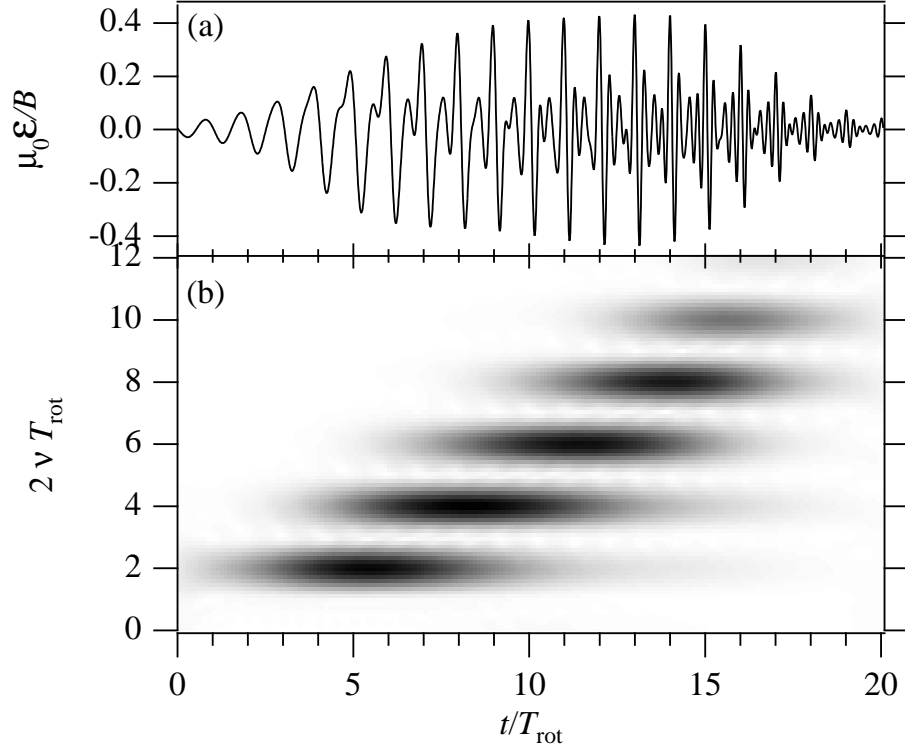


FIG. 6: Same as Fig. 1, but for the optimization of $\langle \cos^2 \theta \rangle$.

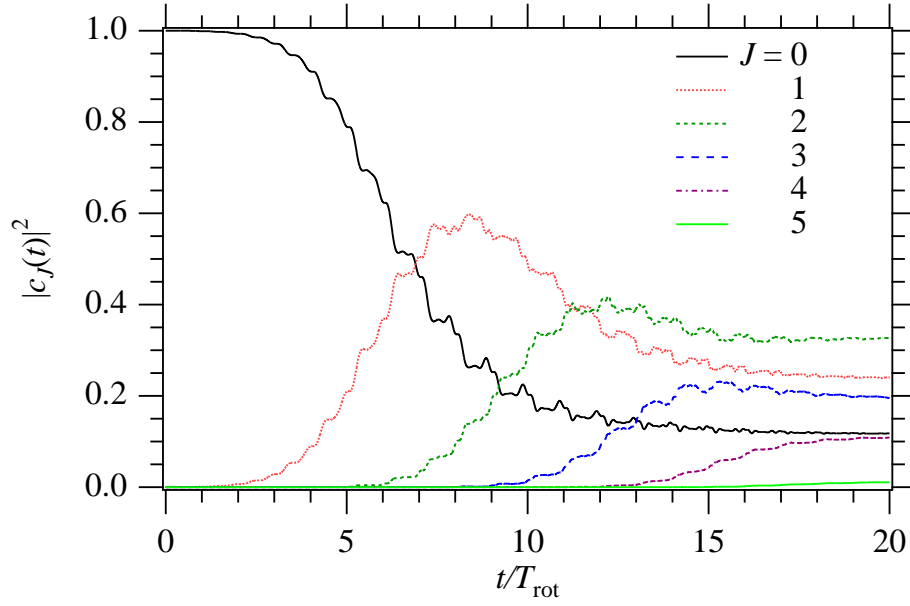


FIG. 7: Time evolution of the population of rotational states of a rigid rotor interacting with the electric field given in Fig. 6(a).

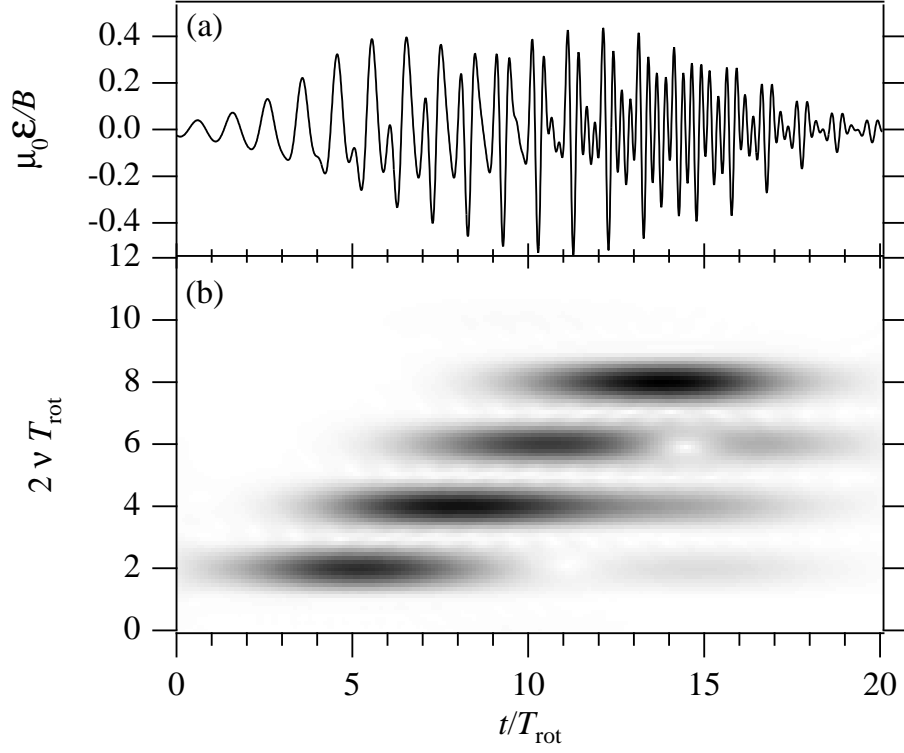


FIG. 8: Same as Fig. 4, but for the optimization of the projection of wave function on the target ψ_{target} corresponding to alignment (see Table I).

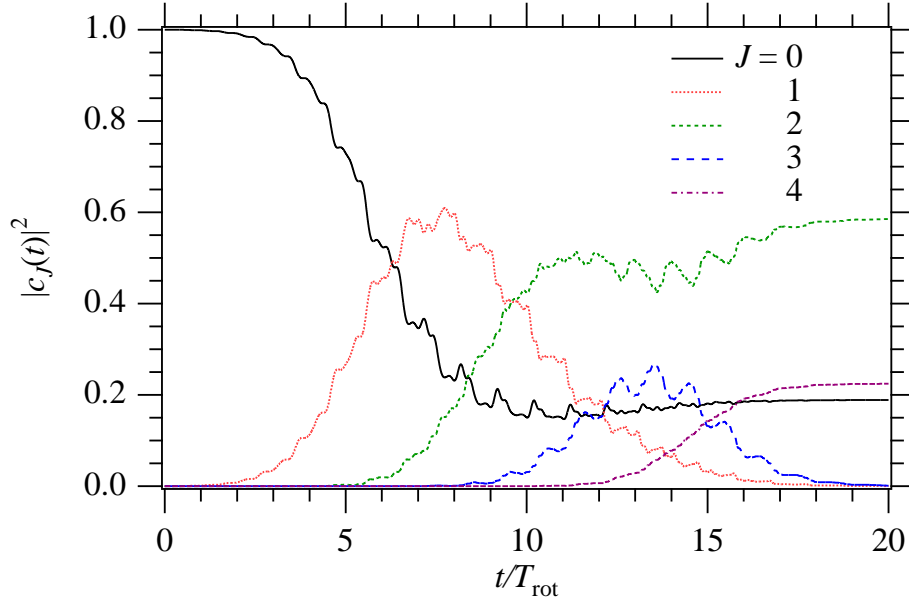


FIG. 9: Time evolution of the population of rotational states of a rigid rotor interacting with the electric field given in Fig. 8(a).

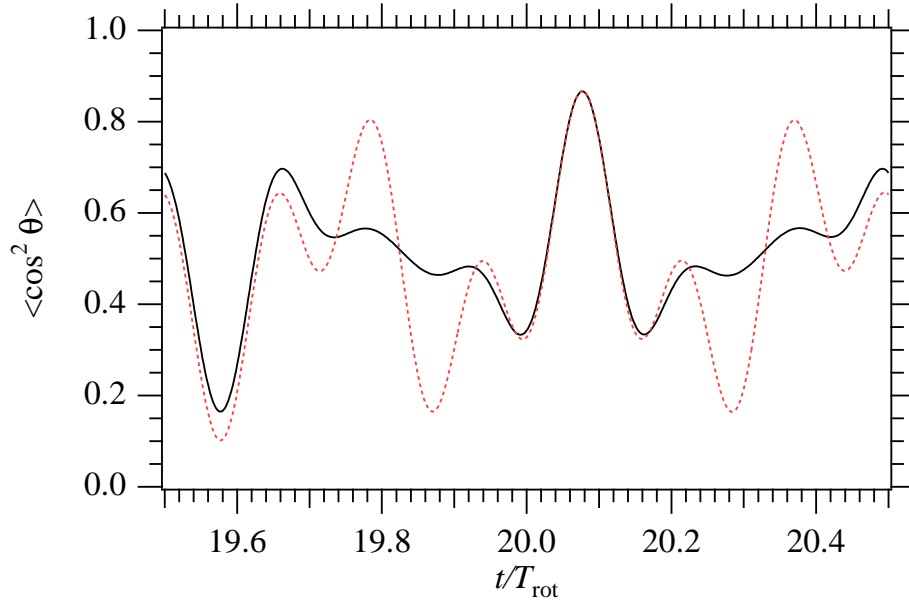


FIG. 10: Alignment, as measured by $\langle \cos^2 \theta \rangle$, obtained for the interaction with the electric field given in Fig. 6(a) (solid line) and Fig. 8(a) (dashed line). The field-free evolution is then periodic with period T_{rot} .

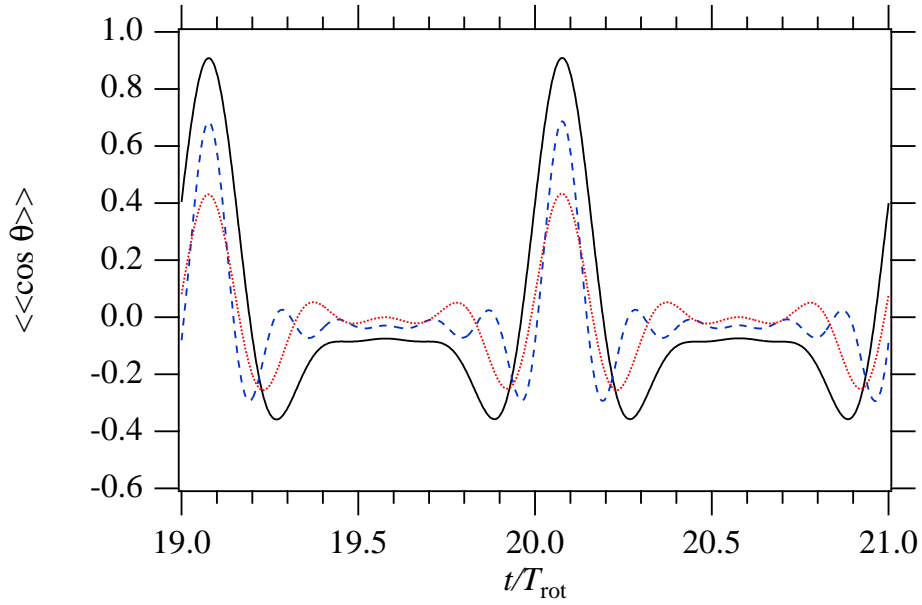


FIG. 11: Orientation, as measured by $\langle \langle \cos \theta \rangle \rangle$, obtained for a rigid rotor interacting with the electric field given in Fig. 1(a), starting from the rotational ground state (solid line) and from a rotational temperature of $k_{\text{B}}T/B \approx 4.77$ (dotted line). For comparison, the orientation obtained with the field optimized for this temperature [Fig. 12(a)] is also shown (dashed line).

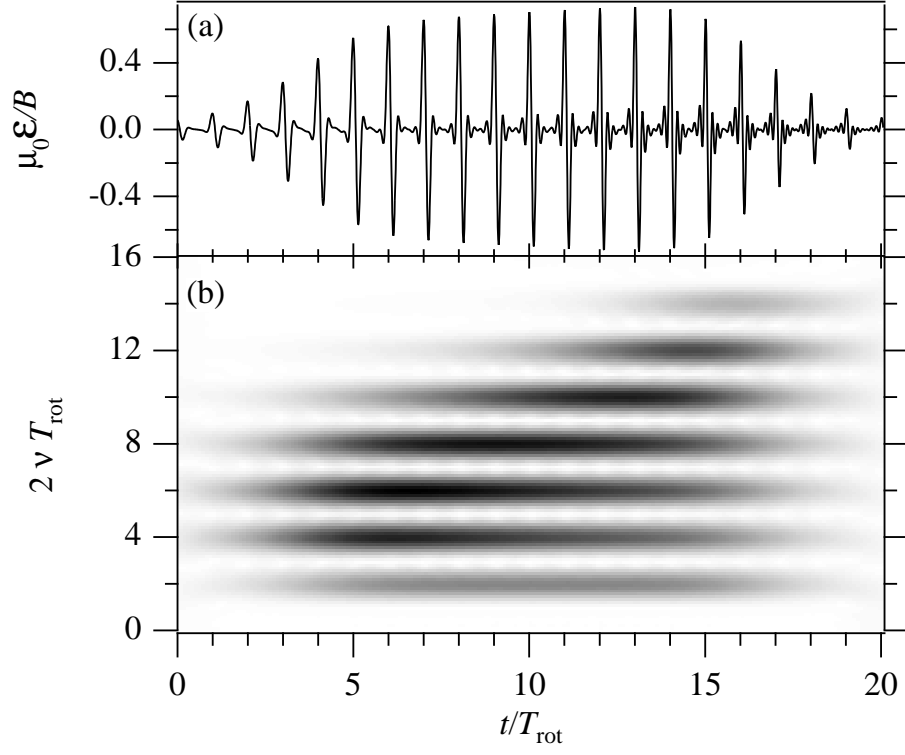


FIG. 12: (a) Electric field obtained for the optimization of $\langle\langle \cos \theta \rangle\rangle$ starting from a rotational temperature of $k_{\text{B}}T/B \approx 4.77$. (b) Short-time Fourier transform of the field in (a).